PHYSICAL REVIEW B **68**, 121305(R) (2003)

Elastic deformation blockade in a single-electron transistor

Norihiko Nishiguchi*
Department of Applied Physics, Hokkaido University, Sapporo 060-8628, Japan
(Received 8 July 2003; published 16 September 2003)

A blockade phenomenon for electron transport in a freely suspended single-electron transistor (SET) is predicted. Voltages applied for its operation induce electromechanical forces acting on the SET, giving rise to structural deformation and collapse over a critical voltage. The electric characteristics become sensitive to charge fluctuations on the SET at the onset of the structural instability, leading to changes in the electrical characteristics that hinder electron transport through the SET around the zero-bias-voltage region.

DOI: 10.1103/PhysRevB.68.121305 PACS number(s): 85.35.Gv, 05.60.Gg, 85.85.+j

Coulomb blockade and single electron tunneling are the fundamental electron transport mechanisms in rigid, motionless nanostructures. These have given rise to single electron transistors as well as various device applications.[1] These mechanisms also govern the transport in nanoelectromechanical systems (NEMS) which incorporate flexible or moveable structural components. The fundamental mechanisms are, however, modified by deformation or by the motion of nanostructures induced by mechanical and/or electromechanical forces, and the modifications depend on the portions of the structure that move. A variety of novel transport characteristics are therefore anticipated in NEMS.[2–9]

Electromechanical effects on electron transport become substantial with increase in flexibility of the systems. The flexibility is determined by the material parameters or the structural geometry, which, however, may vary with the deformation of the structure. Every structure is reversibly deformed by a force smaller than a critical one F_{cr}, and becomes unstable and collapses at F_{cr}.[10] Accordingly, the effective stiffness decreases noticeably as the force approaches F_{cr}, and vanishes at F_{cr}. Considering that electromechanical forces arise because of applied voltages for operation, even subtle electromechanical effects on the transport are expected to be remarkably amplified and novel aspects of the transport phenomena on increasing the voltages are expected to appear. In addition, the collapse of the structure at the critical voltage V_{cr} corresponding to F_{cr} will cause drastic changes in the transport properties. In this Rapid Communication, we show that such amplified electromechanical effects near V_{cr} result in a novel blockade phenomenon for electron transport, taking the case of a freely suspended single electron transistor. We also predict hysteretic behavior in the transport properties related to the collapse of the structure.

Consider a single-electron transistor (SET) consisting of a metal island or a quantum dot fabricated at the center of a freely suspended elastic rectangular beam of length L, width W, and thickness t as shown in Fig. 1. The metal island or the quantum dot are referred to as a *dot* hereafter. When the dot has extra charges with respect to the electrically neutral state or the induced electric dipole, there is an attractive electrostatic force F between the dot and the underlying gate electrode. The force F pushes the elastic beam toward the gate electrode, so that the mutual capacitance C_g between the dot and the gate electrode will increase. Since F depends on the number of excess electrons n, C_g will have a well-defined value, depending on n. The capacitance C_g when an electron tunnels into the dot containing n electrons, as a result, differs from that when another goes out of the dot containing $n+1$ electrons, giving rise to a blockade phenomenon for the transport through the SET as shown below. Here we take C_g and the total capacitance defined by $C_\Sigma = C_1 + C_2 + C_g$ to be a function of n, and denote this dependence as $C_{g,n}$ and $C_{\Sigma,n}$. Assuming that the energy-level separation of electrons in the dot is much smaller than the charging energy e^2/C_Σ, the condition on the bias voltage V, and the gate voltage V_g to allow electron tunneling from the drain to the dot having n electrons becomes

$$C_1 V + C_{g,n} V_g - \left(n + \frac{1}{2} \right) e > 0 \tag{1}$$

for $V > 0$, where $-e$ denotes the electron charge. Equation (1) is derived from the change in the total charging energy for the tunneling event,[11] where the mutual capacitances C_3 between the source and gate electrode and C_4 between the drain and gate electrode do not directly affect the electron tunneling. On the other hand, the condition for electron tunneling from the dot containing $n+1$ electrons to the source is given by

$$[C_2 + C_{g,n+1}] V - C_{g,n+1} V_g + \left(n + \frac{1}{2} \right) e > 0. \tag{2}$$

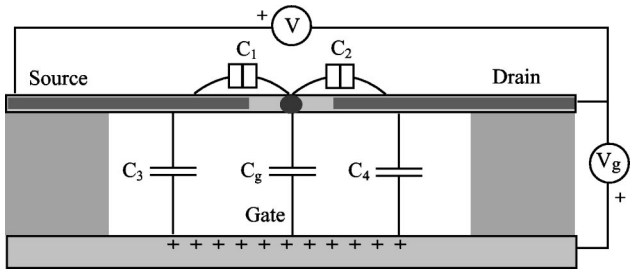

FIG. 1. A SET on a freely suspended elastic beam with an equivalent circuit shown superposed. The beam is separated by the spacers from the underlying gate electrode by distance h. The insulating layer on the gate electrode is omitted in this figure.

The bias voltage V that satisfies both Eqs. (1) and (2) depends on the gate voltage V_g, and has a minimum value V_{th} given by

$$V_{th}^{+}=\frac{\Delta C_{g,n+1}}{C_{\Sigma,n+1}}V_{g,n}^{+} \tag{3}$$

at the gate voltage

$$V_{g,n}^{+}=\frac{C_{\Sigma,n+1}}{[C_1+C_{g,n}][C_2+C_{g,n+1}]-C_1C_2}\left(n+\frac{1}{2}\right)e, \tag{4}$$

where $\Delta C_{g,n+1}\equiv C_{g,n+1}-C_{g,n}$. The same threshold voltage as Eq. (3) is obtained for the case in which the tunneling from the dot to the source occurs first. For $V<0$, the condition for tunneling from the source to the dot having n electrons is

$$-(C_2+C_{g,n})V+C_{g,n}V_g-\left(n+\frac{1}{2}\right)e>0, \tag{5}$$

and that from the dot containing $n+1$ electrons to the drain is

$$-C_1V-C_{g,n+1}V_g+\left(n+\frac{1}{2}\right)e>0, \tag{6}$$

and the threshold voltage becomes

$$V_{th}^{-}=-\frac{\Delta C_{g,n+1}}{C_{\Sigma,n}}V_{g,n}^{-} \tag{7}$$

at the gate voltage

$$V_{g,n}^{-}=\frac{C_{\Sigma,n}}{[C_1+C_{g,n+1}][C_2+C_{g,n}]-C_1C_2}\left(n+\frac{1}{2}\right)e. \tag{8}$$

Because C_g is independent of n for a conventional SET, $V_{th}^{\pm}$ becomes 0 at $V_g=(n+\frac{1}{2})e/C_g$, leading to an $I-V$ curve that does not have a finite bias voltage width for zero-conductance at the gate voltages. The stability diagram for a conventional SET derived from Eqs. (1), (2), (5), and (6) then shows a string of rhombic regions representing zero conductance at $T=0$ K in the $V-V_g$ plane, which are linked to each other at their apexes.[11] On the other hand, $V_{th}^{\pm}$ is expected to be finite for the suspended SET because of the change in C_g with respect to n. Putting $C_{g,n}=C_g(w_n)$ where $C_g(w)=C_g^0/(1+w/h)$, h is the natural distance between the dot and the substrate and w_n is the displacement of the dot having n electrons, the difference in the capacitance can be expressed in terms of the change in the displacement of the dot:

$$\Delta C_{g,n+1}=\frac{w_n-w_{n+1}}{h}\frac{C_g(w_{n+1})C_g(w_n)}{C_g(0)}. \tag{9}$$

It is apparent from Eqs. (3), (7), and (9) that the change of $C_{g,n}$ induced by the dot displacement results in hindering electron transport around the zero bias voltage region, and that the zero-conductance gap widens in proportion to the changes in w_n with respect to n.

In order to derive w_n, one has to pay attention to that the beam is bent not only by the force F between the dot and the gate electrode but also by the force between the source and the gate electrode or that between the drain and the gate electrode. The latter two forces are much larger than F, which dominantly deform the beam. It is, however, hard to rigorously deal with them for the derivation of the beam displacement even for $V=0$. So we introduce a uniform force per unit beam length P averaging the forces except for F over the beam for mathematical convenience. Focusing on the voltage region around zero bias, P can be derived as

$$P(w_n)=-\frac{CV_g^2}{2L(h+w_n)}, \tag{10}$$

where $C=\dfrac{\varepsilon_0 WL}{h}$ and ε_0 is the vacuum dielectric constant, whereas the explicit form of F becomes

$$F_n(w_n)=-\frac{1}{2}\left[\frac{(C_1+C_2)V_g-C_1V+ne}{C_1+C_2+C_g(w_n)}\right]^2\frac{C_g(w_n)^2}{C_g^0h}. \tag{11}$$

Here the subscript n of F_n indicates explicitly the number of excess electrons.

The static beam displacement $w(x)$ is subject to the following differential equation

$$EI\frac{d^4w(x)}{dx^4}=F_n(w_n)\,\delta(x)+P(w_n), \tag{12}$$

where E is Young's modulus, and I the area moment of inertia given by $I=\frac{1}{12}t^3W$. From the solution of Eq. (12) satisfying $w(\pm L/2)=0$ and $w'(\pm L/2)=0$, we obtain the equation for the dot displacement w_n as

$$w_n=\frac{L^3}{192EI}\left[\frac{P(w_n)L}{2}+F_n(w_n)\right], \tag{13}$$

putting $w_n=w(0)$. Dividing F_n into a smoothly varying part $\langle F_n\rangle$ with respect only to V_g and a fluctuation part δF_n, the dominant part w_g of the displacement w_n owing to $\langle F_n\rangle$ and PL yields

$$w_g=\frac{h}{2}\frac{V_{cr}}{V_P}\left[-1+\sqrt{1-\left(\frac{V_g}{V_{cr}}\right)^2}\right], \tag{14}$$

where $V_P=[192EIh^2/(CL^3)]^{1/2}$ and V_{cr} is the critical gate voltage for structural instability of the beam given by

$$V_{cr}=V_P\left[1-2\frac{C_g^0}{C}+8\left(\frac{C_g^0}{C}\right)^2\right]. \tag{15}$$

w_g varies reversibly in the range $[-(h/2)/(V_{cr}/V_P),0]$ for the variations in V_g within $[-V_{cr},V_{cr}]$, as illustrated in Fig. 2. The beam structure becomes unstable at $|V_g|=V_{cr}$, and adheres to the underlying gate electrode for an infinitesimal increase of $|V_g|$. Unless there is charge transfer between the gate electrode and the dot, the beam remains adherent to the gate electrode until the gate voltage is released. The beam

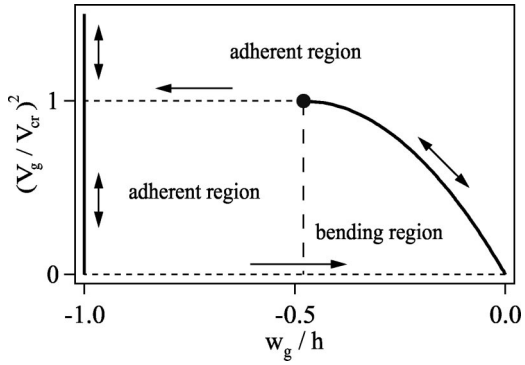

FIG. 2. The displacement w_g versus the gate voltage V_g. The solid circle indicates the critical point at which the beam structure becomes unstable. The arrows denote the direction of reversible or irreversible changes in w_g with respect to V_g. Thickness of the insulating layer on the gate electrode is ignored in this figure. The following Young's modulus and beam dimensions are used for estimation: $E=85.3$ GPa, $L=10\ \mu$m, $t=50$ nm, $W=500$ nm, $h=65$ nm, and $d=6.5$ nm. The effective dielectric constant of the insulating layer is set to be unity for simplicity. The capacitances are $C_\Sigma(0)=140$ aF and $C_g(0)=14$ aF according to the experimental results (Ref. 12) and C_1 and C_2 are assumed to be the same.

displacement shows, as a result, a hysteretic response to the variation of V_g as shown in Fig. 2. We refer to the former gate voltage region as a bending region and to the latter as an adherent region.

The total displacement of the dot w_n can be obtained within the bending region using perturbation theory as

$$w_n = w_g + \frac{h^2}{2V_P^2 C}\,\delta F_n(w_g)\frac{1+\sqrt{1-(V_g/V_{cr})^2}}{\sqrt{1-(V_g/V_{cr})^2}}, \quad (16)$$

and the difference in w_n is given by

$$w_{n+1}-w_n \approx -\frac{eV_g h}{2V_P^2 C}\,\frac{C_g(w_g)^2}{C_\Sigma(w_g)C_g^0}\,\frac{1}{\sqrt{1-(V_g/V_{cr})^2}}. \quad (17)$$

Equations (16) and (17) show that the dot displacement owing to F_n as well as their changes with respect to n are remarkably enhanced near the critical gate voltage due to the softening of the beam. By using Eqs. (9) and (17) and approximating $w_n = w_g$ for C_g and C_Σ, the threshold voltage becomes

$$|V_{th}^{\pm}| \approx \frac{e}{2C}\left[\frac{C_g(w_g)^2}{C_\Sigma(w_g)C_g^0}\right]^2\left(\frac{V_g}{V_P}\right)^2\frac{1}{\sqrt{1-(V_g/V_{cr})^2}}, \quad (18)$$

developing a substantial increase of $|V_{th}^{\pm}|$ with respect to V_g near the critical gate voltage. On the other hand, the transport properties in the adherent region is expected to be the same as those of a conventional SET because C_g becomes a constant for the SET adherent to the gate electrode. Assuming the gate electrode is covered with an insulating layer of thickness d, C_g becomes $C_g(d-h)$, independent of V_g, and the zero threshold bias voltages appear at $V_g=(n+\frac{1}{2})e/C_g(d-h)$.

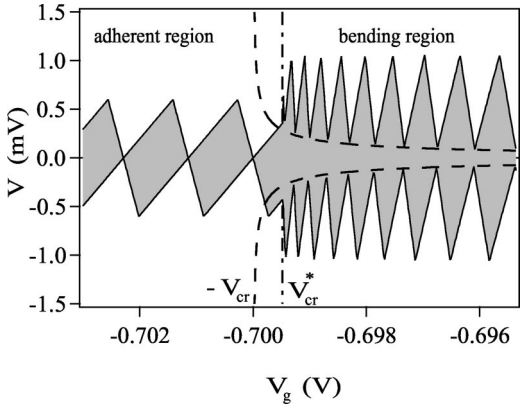

FIG. 3. A stability diagram for the SET shown in Fig. 1. The shaded area is the voltage region where there is no current at $T=0$ K. The minimal voltage for the transport increases with approaching the gate voltage toward the critical gate voltage for the structural instability of the beam. The dashed lines show the threshold bias voltage given by Eq. (18).

We apply the present analysis to a SET on a GaAs beam since such the SETs are fabricated in recent experimental studies.[12,13] The used parameters are listed in the caption of Fig. 2. Figure 3 shows a stability diagram for the SET on a GaAs beam of Fig. 1, which is numerically derived from Eqs. (1), (2), (5), (6), and (13). The shaded area denotes the voltage region where there is no current through the SET at $T=0$ K. Here we note that the structural instability occurs at a gate voltage V_{cr}^* whose magnitude is slightly smaller than V_{cr} predicted by Eq. (15) because the bias voltage induces instability, too. The shaded area consists of overlapping rhombi in the bending region, the intersections becoming the threshold bias voltage for the transport. The threshold bias voltages appear at just the gate voltages that are predicted by Eqs. (4) and (8). The rhombi become narrow as V_g nears the critical gate voltage, owing to the continuous increase in C_g with respect to V_g as understood from Eqs. (4) and (8). At the same time, the conductance gaps between the threshold voltages widen. The widening behavior agrees well with the analytic prediction, Eq. (18), denoted by the dashed lines in Fig. 3. The conductance gaps become substantial near the structural instability, and, therefore, the transport around the zero bias voltage region is definitely hindered by the elastic deformation blockade mechanism.

The stability diagram drastically changes on beam adhesion to the gate electrode. The maximum bias voltage for blockade is reduced in comparison with the rhombi in the bending region because of the increase of C_Σ, whereas the gate voltage width of each rhombus is larger than those in the bending region despite C_g in the adherent region being larger than that in the bending region. The rhombi are linked to each other at their apexes, showing zero threshold bias voltage like conventional SETs. The stability diagram is independent of V_g, and remains unchanged even if V_g is reduced toward 0 because of the hysteretic behavior of the beam displacement as shown in Fig. 2. As a consequence, the stability diagram of Fig. 3 has another plane with only the

rhombi of the adherent region when the gate voltage varies from a magnitude over the critical one to 0.

Finally, we mention dynamic effects on the transport. Although we have assumed static displacement of the beam, at least two dynamic effects are anticipated owing to phonons emerged by the discretely changing force. For every electron tunnel event through the dot, a number of flexural mode phonons will be generated, causing flexural motion of the beam. At an early stage of the vibrations, the generated phonons are almost in phase, therefore we may treat the beam motion classically. The vibrations induce the variation in C_g, which is expected to return its magnitude when an electron entered or went out of the dot, or when the vibration began, and to cause consecutive tunneling. However, the flexural wave is dispersive because of the parabolic dispersion relation with respect to wavenumber,[14] therefore the recovering magnitude in C_g will not occur even if we neglect the decay of vibrations through damping induced by surface defects of the beam, internal friction and phonon emission into the substrate. Another possible dynamic effect is quantum mechanical phonon-assisted tunneling due to the excited phonons, recovering the transport through the SET. A principal frequency of excited flexural mode phonons is $\omega(V_g) = \sqrt{2EI/(\rho A)}[1-(V_g/V_{\rm cr})^2]^{1/4}$ due to the softening. As V_g nears $V_{\rm cr}$, the phonon energy decreases while V_{th}, Eq. (18), increases. Near the critical gate voltage, each phonon has insufficient energy for the phonon assisted tunneling, and the probability of multi-phonon absorption enough for the tunneling will be negligible. Considering these, we may neglect the dynamic effects on the transport.

To conclude, the gate voltage not only directly controls the current flow of a suspended SET but also indirectly affects the transport properties by changing the capacitances via the elastic deformation of the beam. The latter becomes remarkable near the point of structural instability, giving rise to a novel blockade phenomenon as well as to a variational stability diagram with respect to the gate voltage. This new blockade phenomenon and the hysteretic change in the transport characteristics are expected to appear in SETs containing flexible portions such as a SET using a nanowire,[15] a carbon nanotube,[16] or single molecules.[17] These findings should lead to the SET having tunable transport properties on varying the gate voltage, and should usher in new device applications in nanoelectronics.

The author acknowledges Oliver B. Wright for helpful comment on the manuscript. This work was supported by a Grant-in-Aid for Scientific Research (C) from Japan Society for the Promotion of Science (JSPS) (Grant No. 15510109).

*Electronic address: nn@eng.hokudai.ac.jp

[1] M.L. Roukes, *Technical Digest of the 2000 Solid State Sensor and Actuator Workshop* (Transducers Research Foundation, Cleveland, 2000).

[2] M.L. Roukes, cond-mat/0008187 (unpublished).

[3] M.P. Blencowe and M.N. Wybourne, Appl. Phys. Lett. **77**, 3845 (2000).

[4] M.T. Tuominen, R.V. Krotkov, and M.L. Breuer, Phys. Rev. Lett. **83**, 3025 (1999).

[5] A. Erbe, C. Weiss, W. Zwerger, and R.H. Blick, Phys. Rev. Lett. **87**, 096106 (2001).

[6] R. Knobel and A.N. Cleland, Appl. Phys. Lett. **81**, 2258 (2002).

[7] L.Y. Gorelik, A. Isacsson, M.V. Voinova, B. Kasemo, R.I. Shekhter, and M. Jonson, Phys. Rev. Lett. **80**, 4526 (1998).

[8] H. Park, J. Park, A.K.L. Lim, E.H. Anderson, A.P. Alivisatos, and P.L. McEuen, Nature (London) **407**, 57 (2000).

[9] N. Nishiguchi, Phys. Rev. B **65**, 035403 (2001); Phys. Rev. Lett. **89**, 066802 (2002).

[10] F. Yang, J. Appl. Phys. **92**, 2789 (2002).

[11] In *Transport in Nanostructures* (Ref. 1), Chap. 4.

[12] J. Kirschbaum, E.M. Höhberger, R.H. Blick, W. Wegscheider, and M. Bichler, Appl. Phys. Lett. **81**, 280 (2002).

[13] E.M. Höhberger, J. Kirschbaum, R.H. Blick, J.P. Kotthaus, and W. Wegscheider, Physica E **18**, 99 (2003).

[14] N. Nishiguchi, Y. Ando, and M.N. Wybourne, J. Phys.: Condens. Matter **9**, 5751 (1997).

[15] A.T. Tilke, F.C. Simmel, R.H. Blick, H. Lorenz, and J.P. Kotthaus, Prog. Quantum Electron. **25**, 97 (2001).

[16] H.W. Ch. Postma, T. Teepen, Z. Yao, M. Grifoni, and C. Dekker, Science **293**, 76 (2001).

[17] J. Park, A.N. Pasupathy, J.I. Goldsmith, C. Chang, Y. Yaish, J.R. Petta, M. Rinkoski, J.P. Sethna, H.D. Abruña, P.L. McEuen, and D.C. Ralph, Nature (London) **417**, 722 (2002).